Acknowledgment. The author thanks Dr. G. Herzberg for stimulating his interest in Rydberg spectra of NH_4. He also thanks Dr. S. Kato and Y. Kato for assistance in performing the calculations. Calculations were carried out on a M382 computer at the Nagoya University Computational Center and on a M200H computer at the Institute for Molecular Science. This study is supported in part by a Grant-in-Aid for Scientific Research from the Japanese Ministry of Education, Science and Culture.

Registry No. NH_4, 14798-03-9.

Syntheses, Properties, and Molecular and Crystal Structures of $(Me_4N)_4[E_4M_{10}(SPh)_{16}]$ (E = S, Se; M = Zn, Cd): Molecular Supertetrahedral Fragments of the Cubic Metal Chalcogenide Lattice

Ian G. Dance,* Anna Choy, and Marcia L. Scudder

Contribution from the School of Chemistry, University of New South Wales, Kensington, NSW 2033, Australia. *Received October 24, 1983*

Abstract: The complexes $[S_4M_{10}(SPh)_{16}]^{4-}(Me_4N^+)$ (**3M**, M = Zn, Cd) and $[Se_4M_{10}(SPh)_{16}]^{4-}(Me_4N^+)$ (**4M**, M = Zn, Cd) are formed in 80–100% yield by the reactions of sulfur or selenium with the adamantanoid cages $[M_4(SPh)_{10}]^{2-}(Me_4N^+)$ (**2M**, M = Zn, Cd). Complexes **3M** and **4M** do not degrade to the metal chalcogenides, which also are not formed in the preparative reactions under varied conditions. All four complexes **3M** and **4M** are molecular, with the same $(\mu_3\text{-E})_4M_{10}S_{16}$ (E = S, Se) core structure, which is a supertetrahedral fragment of the cubic (sphalerite) ME lattice. In terms of expanding polyhedra the molecular structure is *octahedro*-M_6-*tetrahedro*-$(\mu_3\text{-E})_4$-*truncated tetrahedro*-$(\mu\text{-SPh})_{12}$-*tetrahedro*-M_4-*tetrahedro*-$(SR)_4$, with $\{(\mu_3\text{-E})_2(\mu\text{-SPh})_2\}$ coordination at the six inner metal atoms and $\{(\mu\text{-SPh})_3(SPh)\}$ coordination at the four outer metal atoms. The three-coordinate chalcogenide ions are located at the centers of the hexagonal faces of the $(\mu\text{-S})_{12}$ truncated tetrahedron. By inversion at the sulfur atoms of the 12 bridging thiolate ligands, 186 molecular configurational isomers can occur. Three different crystal structure determinations of **3M** (one Zn, two Cd) have revealed the occurrence of two isomers with $\bar{4}$ molecular symmetry. Crystal structure A (M = Cd), space group $I\bar{4}$, contains one isomer, while the other isomer occurs in crystal structure B (M = Zn), space group $P\bar{4}2_1c$, and crystal structure C (M = Cd), space group $I\bar{4}2m$, which is a mirror disordered form of structure B. Small distortions of the core geometry from idealized $\bar{4}3m$ (T_d) symmetry can be traced to weak repulsions between the phenyl substituents on the surfaces of the molecular anions. Low-frequency infrared and Raman data for **2M**, **3M**, **4M**, and $(Me_4N)_2[M(SPh)_4]$ are interpreted empirically. Crystal data for A: $I\bar{4}$ a = 20.946 (2) Å, c = 14.779 (2) Å, $Z = 2(\times C_{112}H_{128}Cd_{10}S_{20}N_4)$, 2971 reflections ($I > 3\sigma(I)$), Cu K$\alpha$, R (R_w) = 0.033 (0.045). B: $P\bar{4}2_1c$, a = 19.783 (4) Å, c = 16.871 (5) Å, $Z = 2(\times C_{112}H_{128}Zn_{10}S_{20}N_4)$, 1140 reflections, Mo K$\alpha$, R (R_w) = 0.044 (0.054). C: $I\bar{4}2m$, a = 20.140 (2) Å, c = 16.896 (1) Å, $Z = 2(\times C_{112}H_{128}Cd_{10}S_{20}N_4)$, 916 reflections, Mo K$\alpha$, R (R_w) = 0.042 (0.051).

Concentrated and systematic investigation during the past decade has provided detailed description of the formation and chemistry of the class of compounds $[S_wFe_x(SR)_y]^z$, anionic clusters of iron, sulfide (or selenide), and thiolate ions.[1,2] In stark contrast, comparable cluster compounds with metals other than iron were virtually unknown until 1982. The first preparations of $[Fe_4S_4(SR)_4]^{2-}$ (**1**) involved straightforward mixing of the component ions.[3] It was later shown that elemental sulfur[4] or selenium[5] could be used in the formation of **1** or its selenide analogues, in reactions such as (1) containing sufficient thiolate reductant.

$$4FeCl_3 + 14RS^- + 4S \rightarrow [Fe_4S_4(SR)_4]^{2-} + 5RSSR \quad (1)$$

More recently, Holm and co-workers[6] have examined in detail the formation of **1** and complexes $[Fe_2S_2(SR)_4]^{2-}$ from elemental sulfur and have demonstrated the intermediacy of $[Fe(SR)_4]^{2-}$ and $[Fe_4(SR)_{10}]^{2-}$ (**2Fe**). The latter complex ("ferromantane") is a member of a class $[M_4(SR)_{10}]^{2-}$ (**2M**), all with the adamantanoid cage structure.[7,8] The reaction of **2Fe** with sulfur to form **1** (reaction 2, R = Ph) proceeds cleanly, without detectable intermediates or other products, and with 100% yield based on sulfur.

$$[Fe_4(SR)_{10}]^{2-} + 4S \rightarrow [Fe_4S_4(SR)_4]^{2-} + 3RSSR \quad (2)$$

In 1982 we reported extension of the reaction of sulfur plus **2** to include the metals zinc and cadmium and the formation of

(1) Reviews: Holm, R. H. *Acc. Chem. Res.* **1977**, *10*, 427. Holm, R. H. In "Biological Aspects of Inorganic Chemistry"; Addison, A. W., Cullen, W. R., Dolphin, D., James, B. R., Eds.; Wiley: New York 1977, p 71. Ibers, J. A.; Holm, R. H. *Science (Washington, D.C.)* **1980**, *209*, 223. Coucouvanis, D. *Acc. Chem. Res.* **1981**, *14*, 201.

(2) Recent publications: (a) Christou, G.; Garner, C. D. *J. Chem. Soc., Dalton Trans.* **1980**, 2354. (b) Christou, G.; Garner, C. D.; Miller, R. M.; Johnson, C. E.; Rush, J. D. *Ibid.* **1980**, 2363. (c) Armstrong, W. H.; Mascharak, P. K.; Holm, R. H. *J. Am. Chem. Soc.* **1982**, *104*, 4373. (d) Christou, G.; Sabat, M.; Ibers, J. A.; Holm, R. H. *Inorg. Chem.* **1982**, *21*, 3518. (e) Hagen, K. S.; Holm, R. H. *J. Am. Chem. Soc.* **1982**, *104*, 5496. (f) Hagen, K. S.; Christou, G.; Holm, R. H. *Inorg. Chem.* **1983**, *22*, 309. (g) Costa, T.; Dorfman, J.; Hagen, K. S.; Holm, R. H. "Abstracts of Papers", 186th National Meeting of the American Chemical Society, Washington, DC, Aug 1983, American Chemical Society: Washington, DC, 1983; INOR 240. (h) Hagen, K. S.; Watson, A. D.; Holm, R. H. *J. Am. Chem. Soc.* **1983**, *105*, 3905.

(3) Averill, B. A.; Herskovitz, T.; Holm, R. H.; Ibers, J. A. *J. Am. Chem. Soc.* **1973**, *95*, 3523.

(4) Christou, G.; Garner, C. D. *J. Chem. Soc., Dalton Trans.* **1979**, 1093.

(5) Christou, G.; Ridge, B.; Rydon, H. N. *J. Chem. Soc., Dalton Trans.* **1978**, 1423.

(6) Hagen, K. S.; Reynolds, J. G.; Holm, R. H. *J. Am. Chem. Soc.* **1981**, *103*, 4054.

(7) Dance, I. G. *J. Am. Chem. Soc.* **1979**, *101*, 6264.

(8) Hagen, K. S.; Stephan, D. W.; Holm, R. H. *Inorg. Chem.* **1982**, *21*, 3928 and references cited therein.

0002-7863/84/1506-6285$01.50/0

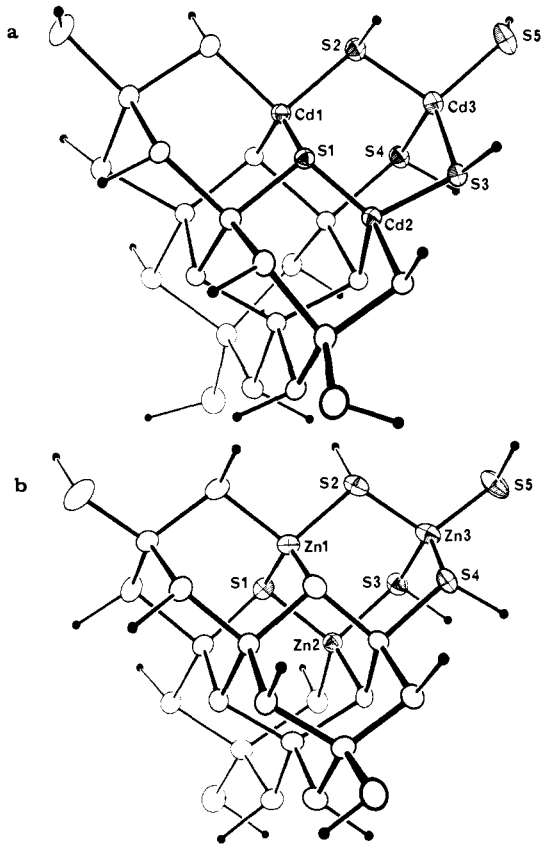

Figure 1. (a) $[S_4Cd_{10}(SPh)_{16}]^{4-}$ ion, structure A. (b) $[S_4Zn_{10}(SPh)_{14}]^{4-}$ ion, structure B (C). The $\bar{4}(S_4)$ axis is vertical, only the first carbon atom of each substituent is included, and the asymmetric unit is labeled.

a different and unprecedented product $(Me_4N)_4[S_4M_{10}(SPh)_{16}]$ (**3M**) (M = Zn, Cd)[9] (see Figure 1). Similar reactions with elemental selenium yield analogous complexes $(Me_4N)_4[Se_4M_{10}(SPh)_{16}]$ (**4M**) (M = Zn, Cd), and so there exists a set of four homologous complexes, $(Me_4N)_4[E_4M_{10}(SPh)_{16}]$ (M = Zn, Cd; E = S (**3**), Se (**4**)). All four anions have the same molecular aggregate structure, based on a supertetrahedral 10-metal section of the cubic (sphalerite) metal chalcogenide ME structure. The 30-atom $E_4M_{10}S_{16}$ core of the ternary chalcogenide metal thiolate aggregate is a symmetrical molecular fragment of the nonmolecular binary metal chalcogenide, the molecular boundary arising by replacement of peripheral chalcogenide ions by thiolate ligands which are doubly bridging or terminal. A similar structure occurs in the $Cd_{10}S_{16}$ core of the aggregate $[Cd_{10}(SCH_2CH_2OH)_{16}]^{4+}$.[10]

This nascent theme of structural congruence of nonmolecular metal sulfides and molecular metal thiolates was developed in the report[11] of the reaction of $[Co_4(SPh)_{10}]^{2-}$ (**2Co**) with HS^- to yield the molecular aggregate $[S_6Co_8(SPh)_8]^{4-}$ (**5**), which is a fragment of the nonmolecular structure of the metal-rich sulfide Co_9S_8, cobalt pentlandite.

In this paper we provide full details of the syntheses and properties of the four complexes **3M** and **4M**. These complexes crystallize (with Me_4N^+) in two different tetragonal forms, one of which is sometimes disordered, and with two different molecular configurational isomers. Full details of the crystal and molecular structures are reported and discussed.

An object of this research was to synthesize the hypothetical anionic aggregate $[SM_8(SPh)_{16}]^{2-}$ (**6M**) (M = Zn, Cd) analogous to $[ClZn_8(SPh)_{16}]^-$ (**7**).[12] Evidence is presented that **6M** is unlikely to be formed in reactions of the type described in this paper.

Experimental Section

All reagents and solvents were research grade (≥98%) and were not further purified. Oxygen was excluded from reaction mixtures and solutions by use of Schlenk and cannula techniques with nitrogen gas: rapid filtrations of well-developed crystals were performed without protection. None of the dry crystalline products decomposes detectably on exposure to laboratory air during 24 h. Powder diffraction measurements were made with a modified Phillips diffractometer; electronic spectra were recorded on a Cary 17 instrument, as 10^{-3} M solutions in distilled acetonitrile; ^{113}Cd NMR spectra were recorded on a Bruker CXP300 spectrometer; solid-state infrared and laser (Ar) Raman spectra were recorded on Perkin-Elmer 580B and Cary 82 instruments, respectively.

$(Me_4N)_2[Zn(SPh)_4]$. To a solution of benzenethiol (22.8 g, 0.207 mol), triethylamine (20.9 g, 0.207 mol), and tetramethylammonium chloride (7.5 g, 0.068 mol) in methanol (80 mL), at room temperature, was added a solution of $Zn(NO_3)_2 \cdot 6H_2O$ (9.0 g, 0.030 mol) in methanol (40 mL). Crystallization was induced in the resulting solution by swirling or seeding and allowed to continue at 0 °C. The colorless crystalline product (10.6 g) was washed with methanol and vacuum-dried. Recrystallization was from a saturated solution in boiling acetonitrile, as large diamond-shaped crystals. Anal. Calcd for $C_{32}H_{44}N_2S_4Zn$: C, 59.10; H, 6.82; N, 4.31. Found: C, 59.13; H, 7.00; N, 4.28.

$(Me_4N)_2[Cd(SPh)_4]$. A solution of $Cd(NO_3)_2 \cdot 4H_2O$ (3.0 g, 10 mmol) in warm propanol (30 mL) was added slowly with stirring to a solution of benzenethiol (7.7 g, 70 mmol) and tributylamine (13.0 g, 70 mmol) in propanol (20 mL). A solution of tetramethylammonium chloride (2.2 g) in methanol (60 mL) was added. The colorless product which crystallized, by seeding if necessary, was filtered, washed with methanol and vacuum-dried. Recrystallization was from a hot saturated solution in acetonitrile. Anal. Calcd for $C_{32}H_{44}N_2S_4Cd$: C, 55.12; H, 6.36; N, 4.02. Found: C, 55.13, H, 6.24; N, 4.20.

$(Me_4N)_2[Zn_4(SPh)_{10}]$. A solution of $Zn(NO_3)_2 \cdot 6H_2O$ (21.0 g, 70.6 mmol) in methanol (70 mL) was added to a well-stirred solution of benzenethiol (20.0 g, 182 mmol) and triethylamine (18.5 g, 182 mmol) in methanol (40 mL) at room temperature. A solution of tetramethylammonium chloride (8.8 g, 80 mmol) in methanol (40 mL) was added with brief stirring to dissolve any precipitate, and the mixture was allowed to crystallize at 0 °C. The colorless crystalline product (24.5 g, 92%) was filtered, washed with methanol, and vacuum-dried. Recrystallization was from acetonitrile plus methanol, with addition of toluene. Anal. Calcd for $C_{68}H_{74}N_2S_{10}Zn_4$: C, 54.40; H, 4.97; N, 1.87. Found: C, 54.32; H, 5.15; N, 1.83.

$(Me_4N)_2[Cd_4(SPh)_{10}]$. A solution of $Cd(NO_3)_2 \cdot 4H_2O$ (21.0 g, 68 mmol) in methanol (60 mL) was added to a well-stirred solution of benzenethiol (20.0 g, 182 mmol) and triethylamine (18.5 g, 182 mmol) in methanol (60 mL) at room temperature, followed by addition of a solution of tetramethylammonium chloride (8.4 g, 77 mmol) in methanol (40 mL). The mixture was stirred only until all precipitate had dissolved, and then allowed to stand undisturbed, finally at 0 °C, while the product (21 g, 73%) crystallized as colorless flakes. The product was washed well with methanol and vacuum-dried. Recrystallization was from acetonitrile (solubility ca. 1 g/mL at room temperature) by addition of toluene. Anal. Calcd for $C_{68}H_{74}N_2S_{10}Cd_4$: C, 48.34; H, 4.41; N, 1.66. Found: C, 48.14; H, 4.61; N, 1.81.

$(Me_4N)_4[S_4Zn_{10}(SPh)_{16}]$. To a solution of $(Me_4N)_2[Zn_4(SPh)_{10}]$ (9.0 g, 6.0 mmol) in acetonitrile (150 mL) at room temperature was added finely powdered sulfur (96.0 mg, 3.0 mmol S) in one portion, and the flask was immediately sealed. The mixture was stirred only until the sulfur had dissolved (ca. 10 min) and then allowed to stand undisturbed at room temperature while the product crystallized as long colorless needles (1.80 g), which were filtered, washed with acetontrile, and vacuum-dried. Anal. Calcd for $C_{112}H_{128}N_4S_{20}Zn_{10}$: C, 47.61; H, 4.57; N, 1.98. Found: C, 47.60; H, 4.79; N, 1.99.

This compound is soluble in DMF, slightly soluble in acetonitrile, and insoluble in acetone, methanol, chloroform, and toluene. Recrystallization can be effected from hot acetonitrile or from DMF plus water.

An alternative preparation of this compound involves DMF, with a higher $S/[Zn_4(SPh)_{10}]^{2-}$ ratio: Powdered sulfur (0.2605 g, 8.1 mmol of S) was added in one portion to a stirred solution of $(Me_4N)_2[Zn_4(SPh)_{10}]$ (7.62 g, 5.1 mmol) in DMF (50 mL) at room temperature. The sulfur dissolved quickly to produce a yellow solution, from which the product subsequently precipitated as a colorless fine powder. This mixture was heated to ca. 70 °C, with addition of the minimum volume of DMF necessary to dissolve the precipitate. Water (ca. 10 mL) was added to the point of incipient crystallization, and crystallization was allowed to proceed slowly. The colorless crystalline product (2.6 g) was filtered, washed with acetone, vacuum-dried, and identified by X-ray diffraction.

(9) Choy, A.; Craig, D.; Dance, I. G.; Scudder, M. L. *J. Chem. Soc., Chem. Commun.* **1982**, 1246.
(10) Strickler, P. *J. Chem. Soc., Chem. Commun.* **1969**, 655.
(11) Christou, G.; Hagen, K. S.; Holm, R. H. *J. Am. Chem. Soc.* **1982**, *104*, 1744.
(12) Dance, I. G. *J. Chem. Soc., Chem. Commun.* **1980**, 818.

Table I. Details of Crystal Structures A, B, and C

	A	B	C
formula, mass	$C_{112}H_{128}Cd_{10}S_{20}N_4$, 3295.5	$C_{112}H_{128}Zn_{10}S_{20}N_4$, 2825.2	$C_{112}H_{128}Cd_{10}S_{20}N_4$, 3295.5
crystal description	{110}{011}{101}{00$\bar{1}$}	{110}{011}{101}{00$\bar{1}$}	
space group	$I\bar{4}$	$P\bar{4}2_1c$	$I\bar{4}2m$
a,b/Å	20.946 (2)	19.783 (4)	20.140 (2)
c/Å	14.779 (2)	16.871 (5)	16.896 (1)
V/Å^3	6484 (1)	6603 (2)	6853.0 (9)
Z	2	2	2
d_{obsd}/g cm^{-3}		1.41 (1)	1.593 (7)
d_{calcd}/g cm^{-3}	1.69	1.42	1.597
temp/°C	21	21	21
radiation λ/Å	Cu Kα, 1.5418	Mo Kα, 0.71069	Mo Kα, 0.71069
scan mode	$\theta/2\theta$	$\theta/2\theta$	$\theta/2\theta$
$2\theta_{max}$/deg	140	40	44
μ/cm^{-1}	165.5	21.74	18.49
crystal dimensions/mm	0.12 × 0.42 × 0.42	0.30 × 0.31 × 0.12	0.20 × 0.20 × 0.24
max, mean, and min transmission coeff	0.274, 0.193, 0.081	0.807, 0.796, 0.778	0.752, 0.734, 0.714
no. of intensity measurements	3392	3468	4467
standard intensity decay	1 → 0.94	nil	1 → 0.93
criterion for obsd refn	$I > 3\sigma(I)$	$I > 3\sigma(I)$	$I > 3\sigma(I)$
no. of independent obsd reflections	2971	1140	916
no. of reflections (m) and variables (n) in final refinement	2971, 327	1140, 183	916, 165
$R = \sum^m\|\Delta F\|/\sum^m\|F_o\|$	0.033	0.044	0.042
$R_w = [\sum^m w\|\Delta F\|^2/\sum^m w\|F_o\|^2]^{1/2}$	0.045	0.054	0.051
$[\sum^m w\|\Delta F\|^2/(m-n)]^{1/2}$	1.65	1.48	1.58

$(Me_4N)_4[S_4Cd_{10}(SPh)_{16}]$. Finely powdered sulfur (0.30 g, 9.4 mmol S) was added in one portion to a well-stirred solution of $(Me_4N)_2[Cd_4(SPh)_{10}]$ (15.0 g, 8.9 mmol) in acetonitrile (50 mL) at a temperature not greater than 20 °C. The mixture was stirred until the sulfur had reacted and dissolved (ca. 20 min). A white crystalline precipitate of the product formed after or during the dissolution of the sulfur. Acetonitrile was added and the mixture heated to 75 °C until all of the product had dissolved; the total volume was ca. 400 mL. The hot solution was allowed to cool slowly, yielding the product as large beautifully formed crystals during a period of 5 days. The product (3.9 g) was washed with acetonitrile and vacuum-dried. Anal. Calcd for $C_{112}H_{128}N_4S_{20}Cd_{10}$: C, 40.82; H, 3.90; N, 1.70. Found: C, 40.59; H, 4.06; N, 1.70. Evaporation of the mother liquor to ca. 70 mL yielded additional microcrystalline product (ca. 3 g) which was isolated similarly.

This compound was prepared also by the following method. Sulfur (0.143 g, 4.5 mmol S), added in one portion to a solution of $(Me_4N)_2[Cd_4(SPh)_{10}]$ (7.37 g, 4.4 mmol) in DMF (30 mL) at room temperature, dissolved quickly. The solution was stirred for a further 30 min; then toluene (10 mL) was added and the solution allowed to stand undisturbed at 20 °C while the product precipitated as colorless microcrystals. After filtration the product (3.35 g) was washed with acetonitrile, vacuum-dried, and identified by X-ray diffraction.

$(Me_4N)_4[S_4Cd_{10}(SPh)_{16}]$ is soluble in DMF and Me_2SO, slightly soluble in acetonitrile, and insoluble in acetone, alcohols, chloroform, and toluene. Recrystallization may be effected from a solution in boiling acetonitrile or from a concentrated solution in DMF at room temperature by careful addition of water, yielding needles. Different crystallographic forms have been obtained from different solutions, as described below. This compound is not decomposed by prolonged refluxing with ethanol or acetonitrile.

$(Me_4N)_4[Se_4Zn_{10}(SPh)_{16}]$. Black selenium powder (0.640 g, 8.1 mmol) was added in one portion to a solution of $(Me_4N)_2[Zn_4(SPh)_{10}]$ (7.60 g, 5.1 mmol) in DMF (50 mL) and stirred at room temperature. Most of the selenium dissolved, generating a yellow-orange solution. After filtration the solution was allowed to stand at room temperature, yielding colorless crystals of the product (2.10 g), which were filtered, washed with acetonitrile, and vacuum-dried. Addition of water to the mother liquor precipitated more of the product, which was washed free of diphenyl disulfide contaminant with acetone; yield 3.0 g. These products were identified by X-ray diffraction.

This compound is soluble in hot DMF, from which it can be recrystallized, but has negligible solubility in hot acetonitrile. Therefore, preparative reactions in acetonitrile, analogous to those successful in the preparations of the other $(Me_4N)_4[E_4M_{10}(SPh)_{16}]$ compounds, are necessarily heterogeneous: the black selenium powder is slowly replaced by the white microcrystalline precipitate of the product.

$(Me_4N)_4[Se_4Cd_{10}(SPh)_{16}]$. Black selenium powder (0.701 g, 8.9 mmol) was added in one portion to a solution of $(Me_4N)_2[Cd_4(SPh)_{10}]$ (15.00 g, 8.9 mmol) in acetonitrile (20 mL) at room temperature, and the mixture was stirred for 3 h, while the selenium was transformed to a white precipitate. The mixture was heated to ca. 75 °C and acetonitrite (ca. 150 mL) added until all solid had dissolved. The pale yellow solution was allowed to cool slowly, yielding the product as well-formed colorless needles (5.4 g) which were washed with acetonitrile and vacuum-dried. Anal. Calcd for $C_{112}H_{128}N_4Se_4S_{16}Cd_{10}$: C, 38.62; H, 3.70; N, 1.61. Found: C, 38.58; H, 3.96; N, 1.74. Recrystallization of this compound can be effected from a solution in hot acetonitrile or from DMF solution by addition of ether.

Polycrystalline X-ray Diffraction. $(Me_4N)_2[Zn_4(SPh)_{10}]$ is isostructural with its cobalt analogue,[7] but $(Me_4N)_2[Cd_4(SPh)_{10}]$, which diffracts poorly, has a different diffraction pattern.[13] As described below, three different crystal structures have been determined for compounds $(Me_4N)_4[S_4M_{10}(SPh)_{16}]$, one (structure C, in space group $I\bar{4}2m$) being a mirror disordered form of another with equivalent dimensions (structure B, space group $P\bar{4}2_1c$), while the third, structure A, occurs in space group $I\bar{4}$ with different dimensions. Therefore there are two different powder patterns, A and B/C, for these three structures, and all compounds $(Me_4N)_4[E_4M_{10}(SPh)_{16}]$ (M = Zn, Cd; E = S, Se), crystallized from different media, have been found to possess one or other of these patterns, which are listed with the supplementary material.[13]

Crystal Structure Determination. All single-crystal measurements were made with a CAD4 diffractometer, using procedures already described.[14] Numerical details for the three crystallographic analyses are presented in Table I. Neutral atom scattering factors for all calculations included anomalous dispersion for Cd, Zn, and S, and were from International Tables.[15] Details specific to each of the structures are presented below.

Crystal Structure A, $(Me_4N)_4[S_4Cd_{10}(SPh)_{16}]$. The crystals for this analysis were obtained by dissolution of the compound (0.1 g) in hot DMF (ca. 1 mL) and addition of water (ca. 0.5 mL), which resulted in the slow growth of well-developed colorless needles. The space group $I\bar{4}$, not being determined by the diffraction symmetry, was confirmed by the successful completion of the structure. Structure solution was by a combination of MULTAN, Patterson, and difference Fourier methods. Least-squares refinement was straightforward. All hydrogen atoms were included in calculated positions (C–H = 1.0 Å), and each was assigned an isotropic temperature factor equivalent to that of the atom to which it was bound. Anisotropic thermal motion was refined for all non-hydrogen atoms. The largest feature on the final difference map was 0.4 eÅ^{-3}. Enantiomer determination was marginally conclusive, with the reported enantiomer allowing slightly improved overall and individual structure factor agreement.

Crystal Structure B, $(Me_4N)_4[S_4Zn_{10}(SPh)_{16}]$. The crystals used in this analysis were needles obtained directly from the preparation in acetonitrile described above. There was visual evidence of parallel multiple growth in some specimens, but the crystal used for data collection was a single fragment. The unit cell for this structure has the

(13) See paragraph at the end of this article regarding supplementary material.

(14) Dance, I. G.; Fitzpatrick, L.; Rae, A. D.; Scudder, M. L. *Inorg. Chem.* **1983**, *22*, 2883.

(15) "International Tables for X-ray Crystallography"; Kynoch Press: Birmingham, England, 1974; Vol. IV, Tables 2.2A and 2.3.1.

Table II. Atomic Coordinates for Non-Hydrogen Atoms

	structure A (Cd)			structure B (Zn)			structure C (Cd)		
	x	*y*	*z*	*x*	*y*	*z*	*x*	*y*	*z*
M1	0.0000	0.0000	−0.1826 (0)	0.0000	0.0000	0.1506 (1)	0.0000	0.0000	0.1632 (1)
M2	−0.0191 (0)	−0.1287 (0)	−0.0036 (0)	0.0533 (1)	0.1166 (1)	0.0000 (1)	0.0548 (1)	0.1207 (1)	0.0007 (1)
M3	−0.1588 (0)	−0.1170 (0)	−0.2058 (0)	0.1830 (1)	0.0703 (1)	0.1614 (1)	0.1923 (1)	0.0744 (1)	0.1731 (1)
S1	0.0636 (1)	−0.0839 (1)	−0.1049 (1)	−0.0357 (2)	0.0954 (2)	0.0847 (2)	−0.0381 (3)	0.1012 (3)	0.0939 (4)
S2	−0.0743 (1)	−0.0572 (1)	−0.2978 (1)	0.0910 (2)	0.0301 (2)	0.2384 (2)	0.0950 (4)	0.0339 (4)	0.2603 (5)
S3	−0.1140 (1)	−0.1889 (1)	−0.0803 (1)	0.1393 (2)	0.1615 (2)	0.0864 (2)	0.1452 (3)	0.1714 (3)	0.0931 (4)
S4	−0.2120 (1)	−0.0295 (1)	−0.1101 (1)	0.2077 (2)	−0.0298 (3)	0.0892 (4)	0.2189 (4)	−0.0305 (3)	0.0939 (4)
S5	−0.2201 (1)	−0.1786 (1)	−0.3203 (2)	0.2711 (3)	0.1104 (2)	0.2350 (3)	0.2886 (5)	0.1124 (4)	0.2503 (6)
C12	−0.0298 (4)	−0.1191 (4)	−0.3498 (6)	0.0635 (8)	0.0987 (8)	0.2990 (10)	0.0667 (13)	0.1037 (13)	0.3167 (18)
C22	0.0003 (5)	−0.1088 (5)	−0.4304 (8)	0.0585 (10)	0.1637 (10)	0.2742 (11)	0.0632 (19)	0.1641 (19)	0.2845 (21)
C32	0.0339 (6)	−0.1574 (7)	−0.4765 (8)	0.0364 (11)	0.2175 (11)	0.3235 (16)	0.0307 (16)	0.2198 (17)	0.3291 (24)
C42	0.0342 (6)	−0.2177 (6)	−0.4427 (9)	0.0198 (11)	0.1973 (13)	0.3986 (14)	0.0174 (19)	0.2146 (20)	0.3999 (23)
C52	0.0045 (7)	−0.2282 (5)	−0.3624 (11)	0.0249 (10)	0.1367 (12)	0.4265 (13)	0.0178 (20)	0.1522 (21)	0.4303 (22)
C62	−0.0267 (7)	−0.1805 (5)	−0.3149 (9)	0.0508 (10)	0.0798 (10)	0.3779 (13)	0.0412 (17)	0.0857 (18)	0.3922 (21)
C13	−0.0918 (4)	−0.2628 (4)	−0.1308 (6)	0.2031 (7)	0.2036 (7)	0.0297 (8)	0.2071 (16)	0.2071	0.0336 (12)
C23	−0.0302 (4)	−0.2851 (4)	−0.1271 (7)	0.1882 (7)	0.2671 (7)	0.0006 (10)	0.1902 (20)	0.2698 (22)	0.0060 (37)
C33	−0.0167 (5)	−0.3461 (5)	−0.1635 (8)	0.2399 (9)	0.3032 (9)	−0.0392 (10)	0.2385 (18)	0.3110 (27)	−0.0425 (27)
C43	−0.0615 (6)	−0.3820 (5)	−0.2012 (10)	0.2988 (9)	0.2735 (9)	−0.0529 (10)	0.2976 (23)	0.2816 (19)	−0.0547 (19)
C53	−0.1256 (5)	−0.3570 (5)	−0.2071 (10)	0.3160 (9)	0.2104 (9)	−0.0277 (11)	0.3177 (11)	0.2147 (19)	−0.0304 (25)
C63	−0.1387 (4)	−0.2982 (4)	−0.1716 (9)	0.2662 (8)	0.1750 (8)	0.0140 (10)	0.2725 (22)	0.1832 (19)	0.0128 (34)
C14	−0.2728 (4)	−0.0733 (4)	−0.0554 (6)	0.2815 (9)	−0.0086 (8)	0.0361 (11)	0.2933 (24)	−0.0071 (37)	0.0449 (38)
C24	−0.2584 (5)	−0.1197 (4)	0.0117 (8)	0.2820 (9)	0.0068 (9)	−0.0428 (11)	0.3495 (18)	0.0011 (22)	0.0730 (19)
C34	−0.3074 (7)	−0.1516 (6)	0.0547 (9)	0.3402 (11)	0.0260 (9)	−0.0834 (12)	0.4061 (17)	0.0218 (17)	0.0268 (21)
C44	−0.3707 (7)	−0.1372 (7)	0.0353 (12)	0.3997 (12)	0.0303 (10)	−0.0423 (16)	0.4049 (21)	0.0428 (21)	−0.0523 (26)
C54	−0.3837 (5)	−0.0947 (9)	−0.0287 (13)	0.4014 (14)	0.0078 (14)	0.0328 (20)	0.3440 (21)	0.0385 (20)	−0.0853 (23)
C64	−0.3356 (5)	−0.0603 (6)	−0.0733 (9)	0.3426 (12)	−0.0108 (11)	0.0768 (13)	0.2813 (28)	0.0100 (35)	−0.0317 (42)
C15	−0.2878 (4)	−0.1351 (4)	−0.3537 (7)	0.3003 (9)	0.0436 (9)	0.2936 (11)	0.3163 (15)	0.0401 (15)	0.3037 (18)
C25	−0.3060 (6)	−0.0774 (5)	−0.3156 (9)	0.2634 (10)	0.0142 (10)	0.3522 (13)	0.2776 (15)	0.0093 (18)	0.3537 (17)
C35	−0.3599 (7)	−0.0465 (6)	−0.3413 (13)	0.2882 (11)	−0.0409 (11)	0.3988 (13)	0.3044 (20)	−0.0456 (18)	0.3982 (22)
C45	−0.3995 (8)	−0.0714 (6)	−0.4053 (14)	0.3505 (13)	−0.0589 (12)	0.3830 (16)	0.3679 (18)	−0.0700 (19)	0.3741 (20)
C55	−0.3837 (8)	−0.1258 (7)	−0.4469 (11)	0.3947 (11)	−0.0308 (12)	0.3291 (17)	0.4046 (17)	−0.0454 (18)	0.3164 (25)
C65	−0.3250 (6)	−0.1587 (6)	−0.4211 (8)	0.3686 (12)	0.0233 (11)	0.2798 (13)	0.3823 (20)	0.0197 (20)	0.2807 (21)
N	−0.3670 (4)	−0.2926 (5)	−0.1847 (9)	0.3212 (8)	0.3081 (8)	0.2389 (10)	0.3148 (11)	−0.3148	−0.2381 (9)
C1N	−0.3268 (9)	−0.2858 (10)	−0.1022 (17)	0.3355 (12)	0.2716 (12)	0.1644 (17)	0.3812 (14)	−0.3487 (14)	−0.2200 (15)
C2N	−0.3256 (11)	−0.3220 (13)	−0.2539 (21)	0.2482 (17)	0.3077 (15)	0.2496 (20)	0.2965 (14)	−0.2453 (15)	−0.2380 (18)
C3N	−0.3911 (8)	−0.2322 (9)	−0.2105 (21)	0.3597 (11)	0.2705 (12)	0.3008 (14)	0.2709 (14)	−0.3251 (14)	−0.1670 (18)
C4N	−0.4185 (8)	−0.3359 (9)	−0.1708 (14)	0.3560 (12)	0.3770 (13)	0.2236 (15)	0.2802 (14)	−0.3464 (14)	−0.3063 (17)

same dimensions (except for differences due to Zn/Cd interchange) as that of structure C, but the cell of structure B is distinguished as being primitive, space group $P\bar{4}2_1c$. A single crystal of the cadmium analogue, obtained from acetonitrile, was also found to have this primitive tetragonal cell, but full diffraction data were not collected. Least-squares refinement proceeded normally. Hydrogen atoms were treated as in structure A. The zinc and sulfur atoms were refined with anisotropic temperature factors; all other non-hydrogen atoms were refined with isotropic temperature factors. On the final difference map the largest peak was 0.6 eÅ^{-3} near Zn1. The enantiomer was clearly differentiated, $[\sum w[\Delta F]^2/(m-n)]^{1/2}$ being 1.48 vs. 1.86.

Crystal Structure C, $(Me_4N)_4[S_4Cd_{10}(SPh)_{16}]$. The crystal for this analysis (which preceded analyses A and B) was from a sample of beautifully formed colorless blocks obtained directly in a preparation using acetonitrile, as described above. Initially the diffraction data were measured and the structure was solved (MULTAN) in a related monoclinic lattice, but then this was transformed on recognition of the tetragonal cell. Consequently multiple measurements of equivalent reflections were available and confirmed unambiguously the presence of the mirror planes in the space group $I\bar{4}2m$, and the 50/50 disorder of the structure in which the molecular point group is $\bar{4}$. (Subsequent examination of additional crystals revealed at least one from this batch which was identical with that reported, and one from a different preparation occurred in space group $P\bar{4}2_1c$, which is $I\bar{4}2m$ without the mirror element and therefore without the 50/50 disorder). During the least-squares refinement anisotropic temperature factors were used only for Cd and S. Two of the phenyl groups lie obliquely across the disordering mirror planes, and during refinement atoms C13 and N were constrained to lie on the mirror plane. Isotropic temperature factors of atoms in two phenyl rings and in the tetramethylammonium cation were not refined. No hydrogen atoms were included. Close examination and testing revealed no evidence of disordering of phenyl groups by inversion at pyramidal sulfur.

The molecules in all three structures possess crystallographic $\bar{4}$ point group symmetry. The same atom labeling scheme is used for all three structures, and is marked on Figures 1 and 4, although the enantiomer of structure A is the inverse of that for structure B (C). Non-hydrogen atom coordinates for the three structures are presented in Table II. Complete tabulations of all atomic parameters and listings of observed and calculated structure factors are deposited with the supplementary material.[13] Thermal vibrational amplitudes are normal. The average (over metal and sulfur atoms) values for the minimum and maximum root-mean-square displacements are 0.19 and 0.23 Å for structure A, 0.19 and 0.26 Å for structure B, and 0.20 and 0.27 Å for structure C.

Results

Preparations and Reactions. High yield preparative methods for the precursor complexes $(Me_4N)_2[M(SPh)_4]$ and $(Me_4N)_2[M_4(SPh)_{10}]$ (**2M**, M = Zn, Cd) are reported in the Experimental Section.

The reactions of elemental sulfur or selenium with solutions of **2M** occur rapidly and cleanly to yield $(Me_4N)_4[E_4M_{10}(SPh)_{16}]$ as the major product. The course of the reaction and the crystallization of the product are dependent on the stoichiometry, solvent system, temperature, and the identity of the chalcogen. A representative reaction is that of $(Me_4N)_2[Cd_4(SPh)_{10}]$ with sulfur in acetonitrile, which is best effected by addition of solid S_8 to a concentrated solution of the precursor at room temperature, with mole ratio S/M = 1/4.[16] The sulfur dissolves and is replaced by a white crystalline precipitate of the product within 20 min. The mixture is then treated with boiling acetonitrile in sufficient volume to dissolve the product, **3Cd**, which crystallizes as large diamond-like crystals on slow cooling. The use of higher proportions of sulfur in this reaction, such as S/M = 2/5 as might be expected from eq 3, leads on heating in acetonitrile to the

$$5[M_4(SPh)_{10}]^{2-} + 8E \rightarrow 2[E_4M_{10}(SPh)_{16}]^{4-} + 8PhSSPh + 2PhS^- \quad (3)$$

formation of a very fine amorphous precipitate which has not yet

(16) For simplification in this discussion all mole ratios are expressed in atomic rather than molecular terms.

been characterized. This complication does not occur if the solvent is DMF, in which large proportions of sulfur (up to S/M = 3/4) can be dissolved with $(Me_4N)_2[Cd_4(SPh)_{10}]$ at room temperature and from which **3Cd** can be isolated in high yield by addition of toluene.

The reaction of $[Zn_4(SPh)_{10}]^{2-}$ with sulfur can be effected similarly, except that the solubilities of the precursor and product (with Me_4N^+) in acetonitrile are lower. A good preparation of **3Zn** can be achieved according to eq 3 in DMF, with addition of water to crystallize the product.

Reactions of black selenium powder with **2M** proceed similarly to those with sulfur, except that the products are slightly less soluble. In acetonitrile there is slow transformation of the selenium to a white microcrystalline precipitate of the product, but the use of DMF permits good homogeneous preparations.

In these reactions of sulfur or selenium with **2M** there is hardly any intermediate development of colors indicative of the formation of polysulfides or polyselenides, and the formation of metal sulfide or selenide has not been observed under any conditions, even heating with excess chalcogen. Consistent with this, the isolated products **3M** and **4M** are thermally stable in solution and solid phases, $(Me_4N)_4[S_4Cd_{10}(SPh)_{16}]$ being unaffected by prolonged refluxing (under dinitrogen) with acetonitrile or ethanol. The crystalline compounds are stable in laboratory atmosphere for several days.

All four compounds **3M** and **4M** are soluble in Me_2SO and DMF and can be recrystallized from the latter by addition of toluene, diethyl ether, or water.

Equation 3 is consistent with the observations on the overall formation reaction. High yields of **3M** and **4M**, 80–100% based on the chalcogen reactant, are readily obtained, indicating the absence of other products containing chalcogenide. Other postulated products, such as $[EM_8(SPh)_{16}]^{2-}$ (**6**) or $[E_2M_{10}(SPh)_{18}]^{2-}$, have not been found in reactions with lower E/M stoichiometry (E/M = 1/8, 2/10, respectively). Consistent also with the occurrence of reaction 3 only is the recovery of the unchanged precursor complex **2M** in reactions with E/M < 4/10 and the isolation only of **3M** or **4M** in reactions with E/M > 4/10. The only complication to an otherwise clean formation of **3M** and **4M** occurs when reactions in acetonitrile with E/M ≥ 4/10 are prematurely heated, generating an insoluble and amorphous product which may be $[M(SPh)_2]_\infty$. Thermal polymerization of $Zn(SPh)_2$ species is known to occur in acetonitrile or alcohol solutions.[17]

Sulfur dissolves in hot acetonitrile solutions of $(Me_4N)_2[Zn(SPh)_4]$, but this complex subsequently crystallizes unchanged.

Crystal Structures. The molecular structure of $[S_4M_{10}(SPh)_{16}]^{4-}$ ion has been obtained from X-ray analysis of crystals of $(Me_4N)_4[S_4Cd_{10}(SPh)_{16}]$ from DMF/H_2O (crystal structure A), $(Me_4N)_4[S_4Zn_{10}(SPh)_{16}]$ from acetonitrile (crystal structure B), and $(Me_4N)_4[S_4Cd_{10}(SPh)_{16}]$ from acetonitrile (crystal structure C). Structures B and C are crystallography isomorphous, but differ in that crystal structure C, in space group $I\bar{4}2m$, is a mirror disordered form of structure B, in space group $P\bar{4}2_1c$. Other than the metrical differences due to the different metals in B and C, there are no substantial crystallographic differences between the refined structures B and C, with the former the more precise.

The two distinct polycrystalline diffraction patterns, for structures A and B/C, allow assignment of one or other of these crystal and molecular structures to all other products **3M** and **4M**. Both zinc complexes, from acetonitrile, DMF, or DMF/H_2O, have been found only with structure B/C, while $(Me_4N)_4[Se_4Cd_{10}(SPh)_{16}]$ from acetonitrile has always crystallized with structure A. $(Me_4N)_4[S_4Cd_{10}(SPh)_{16}]$ crystallizes as B/C from acetonitrile, acetonitrile/toluene, or DMF/toluene, but as structure A from DMF/H_2O. Molecular size (and configuration, see below) rather than solvent properties appear to determine the crystallization behavior.

Molecular Structure and Symmetry. The $[E_4M_{10}(SPh)_{16}]^{4-}$ ion has a molecular structure in which the $M_{10}E_4S_{16}$ core is a ma-

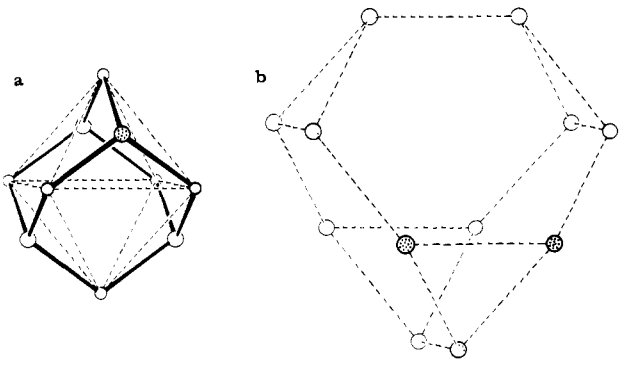

Figure 2. (a) *Octahedro*-$(M_{inner})_6$-*tetrahedro*-$(\mu_3\text{-}S)_4$ core, and (b) the *truncated tetrahedro*-$(\mu\text{-}SR)_{12}$ polyhedra of **3M**, shown with the same scale and orientation.

crotetrahedral fragment of the well-known cubic zinc sulfide (sphalerite) lattice. Each of the 30 metal and chalcogenide atoms has tetrahedral or part-tetrahedral stereochemistry. Six of the metal atoms are arrayed as an inner octahedron, with four of its faces capped by triply bridging chalcogenide ions, E (Figure 2a). The other four faces of the inner M_6 octahedron are capped by podant $\{(\mu\text{-}SPh)_3M\text{-}SPh\}$ groups, the four of which are arrayed as a large outer tetrahedron. Therefore each inner metal atom is coordinated by two triply bridging chalcogenide ions and two doubly bridging thiolate ligands, and each outer metal atom is coordinated by three doubly bridging and one terminal thiolate ligand. The sulfur atoms of the 12 doubly bridging thiolate ligands constitute a tetratruncated tetrahedron (Figure 2b).

The idealized $[E_4M_{10}(SR)_{16}]^{4-}$ structure and its symmetry may be described in terms of expanding polyhedra as *octahedro*-M_6-*tetrahdro*-$(\mu_3\text{-}E)_4$-*truncated tetrahedro*-$(\mu\text{-}SR)_{12}$-*tetrahedro*-M_4-*tetrahedro*-$(SR)_4$. The idealized symmetry of the $M_{10}E_4S_{16}$ core is T_d ($\bar{4}3m$), but this symmetry is necessarily lowered by the thiolate ligand substituents. Each doubly bridging thiolate ligand has pyramidal stereochemistry at sulfur, lowering the maximum symmetry to $T(23)$. The four terminal S–C bonds cannot adhere to the threefold symmetry elements of the core and can maintain no more than $S_4(\bar{4})$ symmetry, which is in fact the crystallographic point group of each of the complete $[S_4M_{10}(SPh)_{16}]^{4-}$ molecules in the three crystals examined.

Configurational Isomerism. Before the dimensions of the three $[S_4M_{10}(SPh)_{16}]^{4-}$ molecules are presented and analyzed, it is appropriate to consider the distributions of ligand substituents over the surfaces of the molecules and to evaluate the molecular configurational isomerism which stems from the pyramidal stereochemistry at each of the 12 bridging thiolates. In molecular thiolate cages of this type the details of core dimensions are influenced in varying degrees by repulsive interactions between contiguous substituents on the molecular surface, and the degree of substituent-induced distortion from idealized geometry correlates inversely with the density of connections in the cage framework.[18] The polycyclic $[E_4M_{10}(SPh)_{16}]$ aggregate possesses the highest degree of connectivity of any thiolate cage investigated to date. The conformations of the substituents at the terminal ligands (due to rotation about M–S and S–C bonds), being energetically subordinate to the configurational stereochemistry at the bridging thiolates, will be disregarded in this analysis which will concentrate on the orientations of the S–C vectors at the bridging thiolates.[19]

With two orientations for each of the 12 doubly bridging S–C bonds at the vertices of the S_{12} truncated tetrahedron, there are $2^{12} = 4096$ microconfigurations for $E_4M_{10}(S\text{–}C)_{12}$, comprising 186 different configurational isomers. The distribution of these isomers among the various point group symmetries is shown in

(17) Dance, I. G. *J. Am. Chem. Soc.* **1980**, *102*, 3445.

(18) Dance, I. G. *Polyhedron*, in press.

(19) This analysis is applicable also to the molecule $M_{10}(SR)_{20}$ which contains triply bridging thiolate ligands in place of the chalcogenide ions in $[E_4M_{10}(SR)_{16}]^{4-}$, because the S–C vectors of the triply bridging thiolates adhere to the T_d point group of the core.

Table III. Configurational Isomers for $E_4M_{10}(S-C)_{12}$

point group	no. of configurational isomers	no. of axis permutations generating microstates	no. of microconfigurations
$T(23)$ chiral	1	1	2
$D_2(222)$ chiral	1	3	6
$C_3(3)$ chiral	7	4	56
$S_4(\bar{4})$ achiral	4	3	24
$C_2(2)$ chiral	8	3	48
$C_1(1)$ chiral	165[b]	12	3960[a]
total	186		4096

[a] Obtained as the balance to total 4096. [b] Obtained as 3960/24.

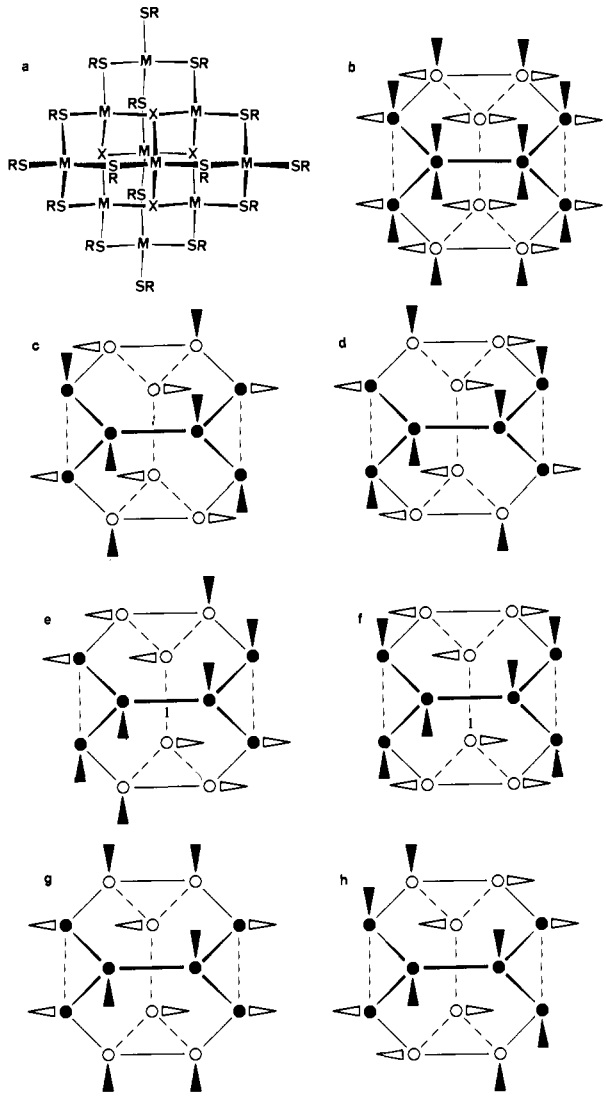

Figure 3. Thiolate substituent configurations. (a) The molecule viewed close to the potential symmetry axis ($\bar{4}$ or 2), defining the 12 bridging thiolate sulfur atom positions, which are shown schematically in (b)–(h) in axial view. (b) The S_{12} truncated tetrahedron of (a), showing the hexagonal faces (full lines and filled circles are above the centroid of the molecule) and both possible orientations of the S–C bond at each thiolate. (c) the 23(T) configuration. (d) The 222(D_2) configuration. (e) The $\bar{4}(S_4)$ configuration, with axial substituents at sulfur positions 1,2,3 around the hexagonal face, structure A. (f) The $\bar{4}$, 1,2,5 isomer. (g) The $\bar{4}$, 1,3,4 isomer, structure B/C. (h) The $\bar{4}$, 1,4,5 isomer.

Table III. Diagrammatic representations of the T, D_2, and four S_4 configurational isomers are presented in Figure 3. The two isomers observed in the three crystal structures both belong to point group S_4, crystal structure A being configurational isomer e, and crystal structures B and C being configurational isomer g of Figure 3. The difference between these two isomers is inversion at one bridging thiolate.

Table IV. Intramolecular Bond Lengths (Å) and Angles (deg) for $[S_4M_{10}(SPh)_{16}]^{4-}$

	A (Cd)	B (Zn)	C (Cd)
M1–S1	2.485 (2)	2.301 (4)	2.472 (6)
M1–S2	2.600 (2)	2.406 (4)	2.612 (8)
M2–S1	2.475 (2)	2.306 (4)	2.477 (7)
M2–S1[3][a]	2.504 (2)	2.301 (4)	2.489 (7)
M2–S3	2.612 (2)	2.411 (4)	2.606 (7)
M2–S4[4]	2.628 (2)	2394 (5)	2.590 (7)
M3–S2	2.558 (2)	2.373 (5)	2.584 (8)
M3–S3	2.567 (2)	2.367 (4)	2.557 (8)
M3–S4	2.569 (2)	2.375 (5)	2.557 (7)
M3–S5	2.486 (3)	2.283 (5)	2.459 (8)
S1–M1–S1[2]	125.0 (1)	122.2 (2)	123.5 (3)
S1–M1–S2	107.3 (1)	108.9 (1)	108.0 (2)
S1–M1–S2[2]	107.9 (1)	105.7 (2)	106.6 (2)
S2–M1–S2[2]	98.2 (1)	104.0 (2)	102.1 (3)
S1–M2–S1[3]	124.1 (1)	122.3 (2)	125.9 (3)
S1–M2–S3	116.9 (1)	103.4 (2)	102.1 (2)
S1–M2–S4[4]	111.6 (1)	112.2 (2)	111.7 (2)
S1[3]–M2–S3	97.4 (1)	112.1 (1)	112.6 (2)
S1[3]–M2–S4[4]	99.3 (1)	101.7 (2)	100.7 (2)
S3–M2–S4[4]	104.6 (1)	103.9 (1)	101.7 (2)
S2–M3–S3	114.7 (1)	105.6 (2)	105.1 (2)
S2–M3–S4	104.1 (1)	99.2 (2)	101.4 (3)
S2–M3–S5	104.5 (1)	113.8 (2)	113.2 (3)
S3–M3–S4	100.3 (1)	115.9 (2)	115.6 (2)
S3–M3–S5	112.1 (1)	107.7 (2)	109.6 (2)
S4–M3–S5	121.4 (1)	114.2 (2)	111.7 (3)
M1–S1–M2	99.9 (1)	102.4 (1)	101.4 (2)
M1–S1–M2[4]	101.8 (1)	102.5 (1)	101.7 (2)
M2–S1–M2[4]	101.5 (1)	102.2 (2)	99.0 (2)
M1–S2–M3	107.0 (1)	108.6 (2)	106.2 (3)
M2–S3–M3	108.0 (1)	107.4 (2)	106.1 (2)
M2[3]–S4–M3	109.9 (1)	109.2 (2)	108.6 (3)
S2–C12	1.771 (8)	1.78 (2)	1.79 (3)
S3–C13	1.782 (8)	1.79 (1)	1.75 (3)
S4–C14	1.766 (9)	1.76 (2)	1.78 (6)
S5–C15	1.756 (10)	1.75 (2)	1.80 (3)
M1–S2–C12	107.8 (3)	108.2 (6)	108 (1)
M3–S2–C12	103.7 (2)	107.1 (6)	107 (1)
M2–S3–C13	113.8 (3)	110.3 (5)	108 (1)
M3–S3–C13	107.6 (3)	112.5 (5)	111 (1)
M2[3]–S4–C14	112.8 (3)	110.5 (7)	114 (2)
M3–S4–C14	101.2 (3)	103.5 (6)	102 (2)
M3–S5–C15	109.8 (3)	107.3 (6)	105 (1)

[a] Symmetry operations: 2 = $-x, -y, z$; 3 = $y, -x, -z$; 4 = $-y, x, -z$.

The configurational isomers can be usefully described in terms of the relative dispositions of thiolate substituents at the six peripheral thiolate sulfur atoms which constitute each hexagonal face of the $(\mu\text{-SR})_{12}$ truncated tetrahedron.[20] Each substituent is axial (ax) to one face and equatorial (eq) to one linked face, and the isomers are distinguished by the arrangements of axial substituents around each S_6 hexagon. In the $T(23)$ isomer the substituents are {ax-1,3,5}; in the $D_2(222)$ isomer they are {ax-1,2,4}; while in the four $S_4(\bar{4})$ isomers they are {ax-1,2,3} occurring in structure A, {ax-1,3,4} in structures B and C, and {ax-1,2,5}, {ax-1,4,5}. The observed isomers are *not* those that maximize the separations of axial substituents, and it is apparent that adjacent axial SPh groups around the hexagonal face do not result in destabilizing steric congestion. Nevertheless, axial pairs of SPh substituents do influence the dimensions of the cage framework.

Molecular Dimensions. Intramolecular bond lengths and angles are presented in Table IV (excluding dimensions of the phenyl substituents and the tetramethylammonium cations, which are unexceptional). The core dimensions can be analyzed statistically in terms of five chemically distinct atom types, M_{inner} (M1, M2), M_{outer} (M3), S^{2-} (S1), $S_{bridging}$ (S2, S3, S4), and $S_{terminal}$ (S5), and therefrom a classification of bond lengths and angles which does

(20) A substituent on the chalcogenide atom centering each face, as in $M_{10}(SR)_{20}$,[19] does not interfere with this description.

Table V. Statistical Analysis of Chemical Classes of Bond Lengths (Å) and Angles (deg) in $[S_4M_{10}(SPh)_{16}]^{4-}$

bonds[a]	Zn	Cd
M_i-S^{2-}	2.303 (3, 0.003)[b]	2.484 (6, 0.012)[b]
M_i-S_{br}	2.404 (3, 0.009)	2.608 (6, 0.013)
M_o-S_{br}	2.373 (3, 0.004)	2.565 (6, 0.011)
M_o-S_t	2.283 (1)	2.473 (2, 0.019)
$M_i-S^{2-}-M_i$	102.3 (3, 0.2)	100.9 (6, 1.2)
$M_i-S_{br}-M_o$	108.4 (3, 0.9)	107.6 (6, 1.5)
$S^{2-}-M_i-S^{2-}$	122.3 (2, 0.1)	124.6 (4, 1.1)
$S^{2-}-M_i-S_{br}$	107.3 (6, 4.4)	106.8 (12, 6.0)
$S_{br}-M_i-S_{br}$	105.7 (5, 6.2)	104.8 (10, 5.8)
$S_{br}-M_o-S_t$	111.9 (3, 3.6)	112.0 (6, 5.5)

[a] $M_i \equiv M_{inner}$; $M_o \equiv M_{outer}$; S_{br} ≡ bridging thiolate; S_t ≡ terminal thiolate. [b] Values quoted: mean (sample size, *sample* standard deviation = $(\sum\Delta^2/(n-1)^{1/2})$. The sample contains only crystallographically independent values.

not break the idealized T_d symmetry of the core. This statistical analysis is presented in Table V, from which important conclusions can be drawn. The bond lengths are precise and valuable in defining the relative sizes of the metal and sulfur atoms of different chemical types and degrees of coordination. There are four distinct M–S distances: referenced to the shortest bond length, {(μ-SPh)$_3$M}–SPh, the increases are (for Zn, Cd, respectively) 0.02 and 0.01 Å in {(μ-SPh)$_2$(μ_3-S)M}–(μ_3-S), 0.09 and 0.09 Å in {(μ-SPh)$_2$(SPh)M}–(μ-SPh), and 0.12 and 0.13 Å in {(μ-SPh)$_1$-(μ_3-S)$_2$M}–(μ-SPh). The increased size of cadmium over zinc ranges from 0.18 Å in {(μ-SPh)$_2$(μ_3-S)M}–(μ_3-S) to 0.20 Å in {(μ-SPh)$_2$(μ_3-S)M}–(μ-SPh).

Bond angles of three types, $M_i-S^{2-}-M_i$, $M_i-S_{br}-M_o$, and $S^{2-}-M_i-S^{2-}$ are clustered closely around their mean values of 101.4°, 107.9°, and 123.8°, respectively, which are essentially independent of the metal identity. Angles of the other three types (Table V), all subtended at a metal by one or two bridging thiolate ligands, range widely and in a manner which is independent of the metal but dependent on the orientations of the thiolate substituents. These angles manifest the repulsive interactions between ligand phenyl groups, which are different for the two configurational isomers.

The types and magnitudes of the distortions from high (T_d) core symmetry, caused by the different lower symmetry arrangements of the ligand substituents, can be evaluated from the core dimensions presented in Table VI. In all three structures the $(S^{2-})_4$ tetrahedra and the $(M_i)_6$ octahedra are regular to within 0.07 Å in 4 Å, but the edges of the S_{12} truncated tetrahedron show differences of up to 0.4 Å in 4 Å. In structure A, with a 1,2,3 distribution of substituents axial to the hexagonal face, the adjacent edges linking axial–axial substituents, namely S2–S3 and S3–S4^4 (see Table VI), are 4.32 and 4.15 Å, whereas the other three crystallographically independent edges average 3.97 Å. Similary, in structures B and C with a 1,3,4 distribution of substituents axial to the hexagonal face, only one edge (S3–S4) links an axial–axial pair, and in both structures this edge is 0.3 Å longer than the mean value of the remainder.

These distortions involve also a slight skewing of the hexagonal faces of the S_{12} polyhedron, revealed as a variation in the radii from the central S^{2-} positions. In Table VI this effect is apparent principally as a slight *shortening* of radii from S1 to the thiolate sulfur atoms involved in an axial–axial substituent pair on an *adjacent* hexagonal face. Thus in structure A there is a shortening of S1–S3^4 (and a corresponding lengthening of S1–S3), while in structures B and C there is a shortening of edges S1–S3 and S1–S4^2.

Molecular plane calculations, reported in Table VII, are used to assess the approach of the molecular $M_{10}S_{20}$ core to different types of higher symmetry, and to evaluate the thiolate bridging geometry. The approach of the $M_{10}S_{20}$ core to the symmetry of point group $T_d(\bar{4}3m)$ can be judged by means of the approach to the mirror operations required of $\bar{4}3m$. The six equivalent mirror elements of $\bar{4}3m$ are represented by two crystallographically independent approaches to mirror operations in crystallographic point group $\bar{4}$. The diagrams of Figure 4 show the quality, which

Table VI. Dimensions (Å) of $S_4M_{10}(S_{br})_{12}$ Polyhedra

	A (Cd)	B (Zn)	C (Cd)
$(S^{2-})_4$ tetrahedron:			
S1–S1^{2a}	4.410 (3)	4.029 (7)	4.356 (12)
S1–S1^3	4.398 (3)	4.036 (7)	4.422 (11)
M_6 octahedron, edges:			
M1–M2	3.798 (1)	3.590 (2)	3.829 (2)
M1–M2^3	3.873 (1)	3.591 (3)	3.846 (2)
M2–M2^3	3.855 (1)	3.587 (2)	3.776 (2)
M_6 octahedron, diagonals:			
M1–M1^3	5.397 (1)	5.082 (3)	5.513 (3)
M2–M2^3	5.450 (1)	5.072 (3)	5.339 (3)
cap to M_6 octahedron:			
M3–M1	4.146 (1)	3.882 (2)	4.156 (2)
M3–M2	4.190 (1)	3.851 (3)	4.126 (3)
M3–M2^3	4.255 (1)	3.888 (3)	4.180 (3)
outer M_4 tetrahedron:			
M3–M3^2	8.262 (1)	7.756 (4)	8.304 (4)
M3–M3^3	8.435 (1)	7.728 (3)	8.289 (3)
$(S_{br})_{12}$ truncated tetrahedron, edges:			
S2–S2^2	3.929 (3)	3.793 (9)	4.063 (15)
S2–S3	4.316 (3)	3.775 (6)	4.083 (10)
S2^2–S4^2	4.043 (3)	3.616 (6)	3.978 (11)
S3–S4 (S3^4–S4^4)	3.943 (3)	4.019 (6)	4.327 (10)
S3–S4^4 (S3^4–S4^2)	4.146 (3)	3.783 (6)	4.030 (10)
$(S_{br})_{12}$ truncated tetrahedron, radii of centered hexagonal face:			
S1–S2	4.097 (3)	3.831 (6)	4.114 (10)
S1–S2^2	4.112 (3)	3.753 (6)	4.077 (10)
S1–S3	4.337 (2)	3.703 (6)	3.954 (10)
S1–S3^4	3.844 (3)	3.909 (6)	4.239 (9)
S1–S4^2	3.912 (2)	3.643 (6)	3.910((11)
S1–S4^4	4.220 (3)	3.902 (6)	4.195 (9)

[a] Symmetry operations: 2 = $-x, -y, z$; 3 = $y, -x, -z$; 4 = $-y, x, -z$.

is better in structures B and C, of the approximate mirror operation (neglecting the thiolate substituents) parallel to the $\bar{4}$ axis. The other independent approach to a mirror operation of this type is not apparent from the figures and is reported quantitatively in part 3 of Table VII. In structures B and C the displacements of atoms supposedly on or mirrored by the best plane agree generally to within 0.05 Å, while in structure A the general agreement is ca. 0.1 Å with discrepancies up to 0.4 Å.

In addition to these approximate molecular mirror operations, there exist in the $M_{10}S_{20}$ core almost parallel sets of almost coplanar atoms, which are related to the planes of the cubic close packed lattice of which the $M_{10}S_{20}$ core is a molecular fragment. Part 1 of Table VII describes the series of layers normal to the pseudothreefold axis. The hexagonal $(S_{br})_6$ face of the truncated tetrahedron is planar (plane I, Table VII, mean displacement 0.12 Å for all three structures), with the central S^{2-} lying slightly outside the face (0.15 Å for Zn, 0.19 Å for Cd).[21] The M_6 and S_6 layers (planes II and III, Table VII) are also planar (mean displacements 0.06 and 0.03 Å, respectively) and parallel (within 4°) to the hexagonal face. The smaller M_3 and $(S_{br})_3$ layers are parallel to the larger layers.

The $M_{10}S_{20}$ core also contains two crystallographically equivalent layers of six sulfur atoms, $(S_{br})_4(S^{2-})_2$, normal to the $\bar{4}$ molecular axis (see Figure 1 and Table VII, part 2). These six atoms are closely coplanar (mean displacement 0.02 Å) in structures B and C, but in structure A (mean displacement 0.18 Å) there is a twisting of the layer, mainly at S3, concomitant with the centering of the triplet of three contiguous axial substituents at S3 in structure A.

Part 4 of Table VII defines the orientations of the bridging thiolate substituents relative to the MSM bridge, which are not unusual.

In summary of the molecular symmetry of the $[S_4M_{10}(SPh)_{16}]^{4-}$ ions, the central highly connected $S_4M_{10}(S_{br})_{12}$ core of the structure

(21) Larger structural distortions occur at the terminal thiolate ligands, manifest as larger displacements of S_t(S5) from the hexagonal face, particularly in structure A.

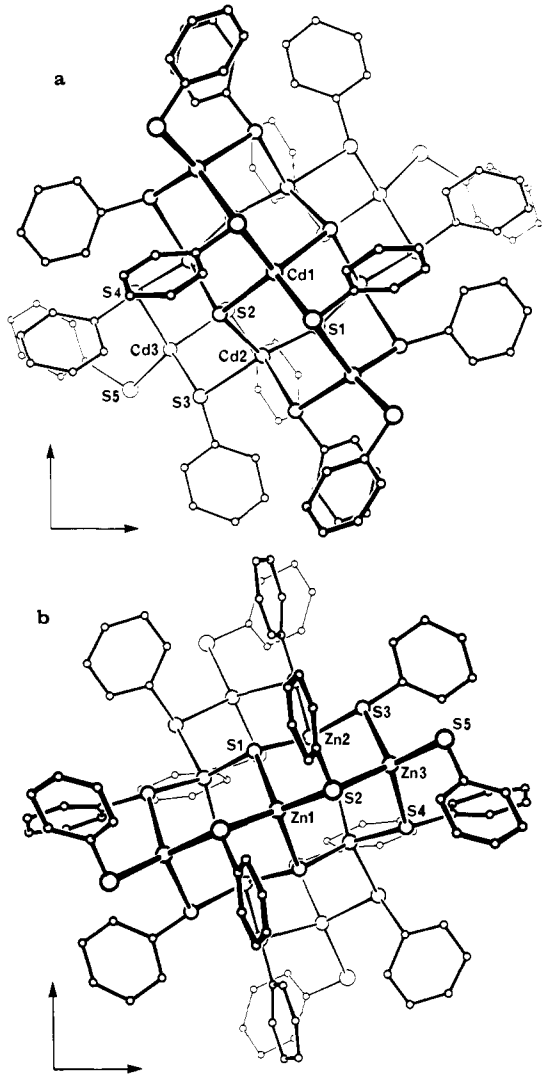

Figure 4. $[S_4M_{10}(SPh)_{16}]^{4-}$ **3M** viewed along the $\bar{4}$ axis: (a) M = Cd, structure A; (b) M = Zn, structure B.

closely approximates the high symmetry of point group $\bar{4}3m$ and the parallel planar layers of a 26-atom molecular fragment of the cubic nonmolecular sphalerite lattice. Within this core the deviations from these idealizations are fully attributable to the lower symmetry imposed by the substituents at the bridging thiolates, the deviations being larger in structure A. The sulfur atoms of the terminal thiolates, being less connected, are more variable in location.

Vibrational Spectra. Infrared and Raman spectra have been measured at room temperature for solid samples of the seven compounds $(Me_4N)_2[M(SPh)_4]$, **2M**, **3M** (M = Zn, Cd), and **4Cd**. The spectra all contain well-resolved and relatively narrow bands (width at half-intensity ca. 10 cm^{-1} Raman, 10–20 cm^{-1} infrared). The results for the significant low-frequency region (400 cm^{-1}) where the spectra are dependent on the structure type and the identity of the metal or chalcogen are presented comparatively in Figure 5.

These spectra provide valuable reference for symmetrical cage compounds of known structure. At this stage our analysis is empirical: it is possible to associate frequency regions with structural moieties, but the information available does not allow unambiguous assignment of frequencies to vibrational modes. There are two well-defined frequency regions in $[M(SPh)_4]^{2-}$: region I, 160–210 cm^{-1}; region II, 315–375 cm^{-1}. Both of these regions occur also, but with slightly reduced frequencies, in the complexes **2M** (I, 155–200; II, 320–370 cm^{-1}) and **3M** and **4Cd** (I, 145–200; II, 290–350 cm^{-1}). In both of these regions the frequencies of the cadmium compounds are 5–20 cm^{-1} lower than those of the zinc homologues. It can be concluded that M–SPh

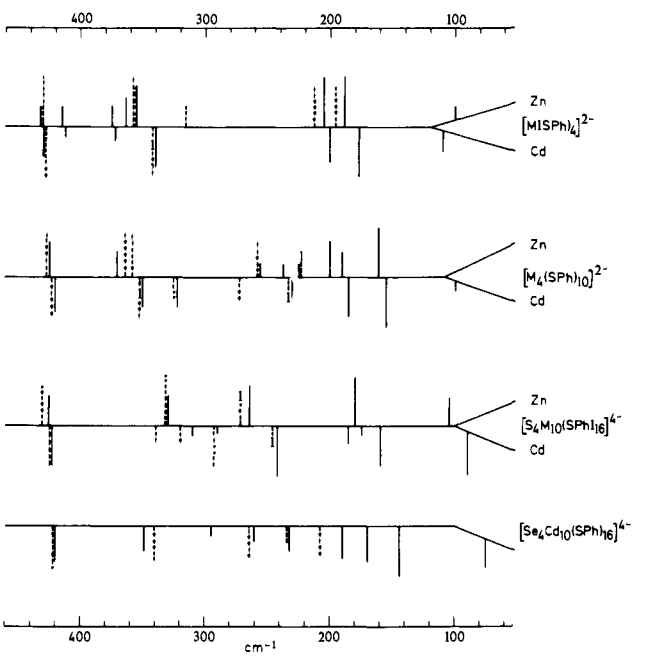

Figure 5. Raman (solid lines) and infrared (broken lines) frequencies below 440 cm^{-1} for the seven compounds marked. Low-frequency limits are 50 cm^{-1} (Raman), 200 cm^{-1} (IR). The relative intensities marked are approximately proportional to optical density, emphasizing weaker lines.

vibrations of terminal ligands occur in both frequency regions.

An additional frequency (region III, 220–275 cm^{-1}) occurs in the compounds **2M** and is probably associated with the bridging thiolate ligands. The frequencies are not clearly lower for cadmium than for zinc.

The vibrational spectra of the complexes **3M** are not more complex or markedly different from those of **2M**, which is consistent with the adamantane basis of both structure types, and the same M,S atoms in the aggregate core. We conclude that there are no additional frequencies assignable to vibrations with substantial $(\mu_3\text{-S})M_3$ character and that the $(\mu_3\text{-S})M_3$ moiety in **3M** is vibrationally very similar to the $(\mu\text{-SPh})M_2$ moiety in **2M**. The spectrum of **4Cd** is more complex than that of **3Cd** and can be interpreted (see below) in terms of additional frequencies characteristic of the $(\mu_3\text{-Se})Cd_3$ moiety.

Closer examination of the spectra of **3M** shows that bands in the central region III are at slightly higher frequency than those in **2M**. For instance, 223–256 cm^{-1} in **2Zn** corresponds with 265–273 cm^{-1} in **3Zn**, and the pattern 230 (R), 235 (IR) in **2Cd** corresponds with the pattern 242 (R), 246 (IR), 293 (IR) in **3Cd**. The metal participation is clearly indicated by the relationships 330 (IR, R)/293 (IR) 290 (R), and 273 (IR) 265 (R)/246 (IR) 242 (R), and 180 (R)/160 (R) for Zn/Cd in **3M**.

The spectrum of **4Cd** contains more frequencies in the central region III than that of **3Cd**, and several fairly clear shifts to lower frequency are apparent: 293 (IR) 290 (R)/264 (IR) 260 (R), and 246 (IR) 242 (R)/235 (IR) 232 (R), and 160 (R)/145 (R), and 90 (R)/76 (R) for S/Se in $[E_4Cd_{10}(SPh)_{16}]^{4-}$. We suggest, tentatively, that frequencies in the 250–300-cm^{-1} region are characteristic of $(\mu\text{-SPh})Cd_2$ and in the 200–240-cm^{-1} region are characteristic of $(\mu_3\text{-Se})Cd_3$ in **4Cd**.

Further analysis of the vibrational behavior of these large symmetrical molecules will require additional data from different phases and the support of theoretical models. Our assignments are consistent with those made for other systems. The closest comparison compound is $[Cd_{10}(SCH_2CH_2OH)_{16}]^{4+}$, where there are two important bands at 197 and 160 cm^{-1} assigned as being largely Cd–S stretching vibrations.[22] In the structurally characterized molecular cages $[Cu_4(SPh)_6]^{2-}$ and $[M_5(SPh)_7]^{2-}$ (M

(22) Haberkorn, R. A.; Que, L., Jr.; Gillum, W. O.; Holm, R. H.; Liu, C. S.; Lord, R. C. *Inorg. Chem.* **1976**, *15*, 2408.

Table VII. Molecular Planes for $[S_4M_{10}(SPh)_{16}]^{4-}$

Part 1. Planes normal to the pseudothreefold axis: successive layers of the pseudo cubic close packing

	A (Cd)	B (Zn)	C (Cd)		A (Cd)	B (Zn)	C (Cd)
Plane I: centered hexagonal face of the truncated tetrahedron:				Plane III: $(\mu_3\text{-S})_3(S_{br})_3$ layer			
	$(\mu_3\text{-S})(S_{br})_6 + (S_t)_3$ layer			$S1^1$	+0.08	−0.02	0.00
(S1)[a]	(+0.19[b])[a]	(+0.15[b])[a]	(+0.19[b])[a]	$S1^3$	−0.02	−0.03	−0.04
S2	+0.20	−0.13	−0.12	$S1^4$	+0.04	−0.01	−0.01
$S2^2$[c]	−0.12	−0.04	−0.06	S4	−0.03	+0.03	+0.02
$S4^2$	−0.08	+0.14	+0.15	$S3^2$	−0.06	+0.01	0.00
$S3^4$	+0.18	−0.07	−0.06	$S2^4$	−0.01	+0.02	+0.03
$S4^4$	−0.09	−0.11	−0.11				
S3	−0.10	+0.21	+0.20	Plane IV: $(M_i)_3$ layer: $M2^2$, $M1^3$, $M2^3$			
(S5)	(+0.84)	(+0.07)	(−0.12)	Plane V: $(S_{br})_3$ layer: $S2^3$, $S3^3$, $S4^3$			
($S5^2$)	(−0.38)	(−0.31)	(−0.24)				
($S5^4$)	(−0.42)	(+0.30)	(+0.39)				
	Plane II: $(M_i)_3(M_o)_3$ layer						
M1	+0.11	−0.05	−0.04				
M2	+0.02	−0.07	−0.09				
$M2^4$	+0.08	−0.05	−0.08				
M3	−0.07	+0.06	+0.06				
$M3^2$	−0.09	+0.05	+0.06				
$M3^4$	−0.05	+0.06	+0.08				

Angles (deg) between planes: the three values quoted are for structures A, B, and C, respectively

planes	II	III	IV	V
I	4.0, 1.9, 1.9	3.7, 1.8, 1.6	2.9, 1.6, 1.1	3.6, 1.3, 0.8
II		0.4, 0.1, 0.3	1.5, 0.4, 1.0	1.3, 0.8, 1.4
III			1.3, 0.4, 0.8	1.2, 0.7, 1.2
IV				0.6, 0.3, 0.4

Part 2. S_6 layer normal to $\bar{4}$ axis

atom	A	B	C
S1	−0.10	−0.04	+0.01
$S1^2$	−0.10	−0.04	+0.01
S3	+0.27	−0.01	−0.01
$S3^2$	+0.27	−0.01	−0.01
S4	−0.17	+0.04	0.00
$S4^2$	−0.17	+0.04	0.00

Part 3. Pseudomirror operation for the $M_{10}S_{20}$ core (required of point group $\bar{4}3m$)[d]

atom	A (Cd)	B (Zn)	C (Cd)	atom	A (Cd)	B (Zn)	C (Cd)
$M2^4$	−0.08	+0.02	+0.01	($S3^2$)	(−2.36)	(−1.81)	(−1.93)
$S4^2$	+0.11	+0.27	+0.26	(M1)	(+1.82)	(+1.81)	(+1.97)
$S3^4$	+0.43	−0.17	−0.23	($M2^2$)	(−1.97)	(−1.78)	(−1.86)
$M3^2$	−0.12	0.00	+0.01	(M2)	(+2.03)	(+1.79)	(+1.90)
$M3^4$	+0.03	0.00	−0.01	($M1^3$)	(−1.84)	(−1.80)	(−1.95)
$S5^2$	−0.06	−0.13	−0.12	S(4)	(+2.08)	(+1.88)	(+2.01)
$S5^4$	−0.34	0.02	+0.09	($S3^3$)	(−2.06)	(−1.88)	(−1.99)
$S1^2$	−0.07	+0.01	+0.05	(M3)	(+4.23)	(+3.88)	(+4.16)
$S1^3$	+0.12	−0.01	−0.04	($M3^3$)	(−4.19)	(−3.85)	(−4.13)
$M2^3$	−0.01	−0.01	−0.01	(S2)	(+4.04)	(+3.76)	(+4.12)
(S1)[a]	(+2.15)[a]	(+2.03)[a]	(+2.22)[a]	($S4^3$)	(−4.25)	(−3.87)	(−4.13)
($S1^4$)	(−2.24)	(−2.01)	(−2.20)	(S3)	(+3.95)	(+3.89)	(+4.18)
($S4^4$)	(+2.02)	(+1.75)	(+1.89)	($S2^3$)	(−3.98)	(−3.83)	(−4.15)
($S2^4$)	(−2.02)	(−1.86)	(−2.08)	(S5)	(+6.47)	(+5.77)	(+6.14)
($S2^2$)	(+1.92)	(+1.96)	(+.2.14)	($S5^3$)	(−6.11)	(−5.63)	(−6.08)

Part 4. Angles (deg) at doubly bridging thiolate

S_q	A	B	C	S_q	A	B	C
	Inclination of the S_q–Cl_q vector to the M–S_q–M bridge plane				Angle between SC_6H_5 plane and bridged M–M vector		
S2	62.7	58.7	59.8	S2	58.3	73.5	69.9
S3	52.9	51.9	56.3	S3	30.6	48.0	48.6
S4	58.6	59.4	57.5	S4	80.2	47.1	45.4

[a] Values are atom displacements (Å) from least-squares planes: atoms in parentheses were not included in the least-squares calculation. [b] The positive displacement is outside the polyhedron face. [c] Symmetry operations: 2 = −x, −y, z; 3 = y, −x, −z; 4 = −y, x, −z. [d] As the molecular point group is crystallographic $\bar{4}$, there are two crystallographically independent mirror operations of this type for each structure. The other is shown in Figure 4.

= Cu, Ag) the main M–SPh stretching vibrations are 150–250 cm^{-1} (Cu) and 140–210 cm^{-1} (Ag).[23] In the compounds $M(SPh)_2$ and $M(S\text{-}t\text{-}Bu)_2$, with unknown but probably nonmolecular structures, the frequencies most associated with M–SR stretching are at 180–210 cm^{-1} (Zn) and 170–200 cm^{-1} (Cd).[24,25] In $[Au(SPh)_2]^-$ there are Au–SPh (presumably terminal) frequencies (IR,R) 230–260 cm^{-1}, while in AuSPh (bridging ligands presumed) the IR frequencies are 219 and191 cm^{-1}.[26]

(23) Bowmaker, G. A.; Tan, L. C. *Aust. J. Chem.* **1979**, *32*, 1443.

(24) Canty, A. J.; Kishimoto, R.; Deacon, G. B.; Farquharson, G. J. *Inorg. Chim. Acta* **1976**, *20*, 161.

(25) Said, F. F.; Tuck, D. G. *Inorg. Chim. Acta* **1982**, *59*, 1.

Electronic Absorption Spectra. In acetonitrile solution the zinc and cadmium compounds $[M(SPh)_4]^{2-}$, **2M**, **3M**, and **4M** absorb only in the ultraviolet region. The absorption envelopes are poorly resolved but show features which can be associated with terminal and doubly bridging benzenethiolate ligands, and (at 32–35 × 10^3 cm^{-1}) with the $\{(\mu_3\text{-S})Cd_3\}$ function in **3Cd**. These features occur at lower energy when the metal is cadmium or the chalcogenide is selenide, as expected. Absorption associated with the $\{(\mu_3\text{-E})M_3\}$ function is at ca. 1 eV higher energy than the band gap in the corresponding metal chalcogenide, ME.[27] Details of the electronic spectra of these systems are to be published separately.

Discussion

Reactions 3 leading directly and quantitatively from **2M** to complexes **3M** and **4M** (M = Zn, Cd) are unique as the only instances of chalcogen plus metal–thiolate preparative methods for metals other than iron. The absence of alternative products or of intermediates is characteristic also of reaction 2 of $[Fe_4(SPh)_{10}]^{2-}$ with sulfur. Similar reactions with iron precursors are (4) (R = Ph,[6] Et),[2e,h] (5),[2e,h] and (6).[2e,h,28]

$$2[Fe(SR)_4]^{2-} + 2S \rightarrow [Fe_2S_2(SR)_4]^{2-} + RSSR + 2RS^- \quad (4)$$

$$[Fe_2(SEt)_6]^{2-} + 2S \rightarrow [Fe_2S_2(SEt)_4]^{2-} \quad (5)[28]$$

$$3[Fe(SEt)_4]^{2-} + 4S \rightarrow [Fe_3S_4(SEt)_4]^{3-} \quad (6)[28]$$

The significance of this simple route to **3M** and **4M** derives from reports[11,29] of failures of standard procedures for the synthesis of $[S_wM_x(SR)_y]^{z-}$ for first transitions series metals other than iron. The most closely related reaction, from **2Co** to yield **5** (eq 7[11]), involves substitution, not the reduction of chalcogen by thiolate as in the reactions discussed above.

$$2[Co_4(SPh)_{10}]^{2-} + 6HS^- \rightarrow [S_6Co_8(SPh)_8]^{4-} + 6PhSH + 6PhS^- \quad (7)$$

Some related reactions have been described. Lead thiolates $[Pb(SR)_2]_p$ are rapidly converted to the lead chalcogenide on treatment with sulfur or selenium.[30] Reaction of $[Fe(SPh)_4]^{2-}$ with dibenzyl trisulfide yields $[Fe_2S_2(SPh)_4]^{2-}$ and other products,[31,32] while sulfur insertion into chelated thiolates is well established.[33]

All evidence accords with high thermodynamic stability for **3M** and **4M** relative to degradation to alternative metal chalcogenide or metal thiolate products. It is remarkable that the disproportionation (8) to form two products of established stability does

$$2[E_4M_{10}(SPh)_6]^{4-} \rightarrow 8ME + 3[M_4(SPh)_{10}]^{2-} + 2PhS^- \quad (8)$$

not occur during prolonged reflux of acetonitrile solution. Neither is the metal chalcogenide formed in the presence of excess chalcogen, and the complexes are hydrolytically stable. The symmetric linkage of 10 coordination tetrahedra in the structure apparently contributes a substantial molecular "lattice" energy. Complexes **3M** react with electrophiles of various types.[34]

The preferred formation of **3M** appears to preclude the preparation of $[SM_8(SPh)_{16}]^{2-}$ **6M** by reaction 9 of **2M** with sulfur.

$$2[M_4(SPh)_{10}]^{2-} + S \rightarrow [SM_8(SPh)_{16}]^{2-} + PhSSPh + 2PhS^- \quad (9)$$

Molecules **3M** and **4M** do not contain any metal–metal bonding, the aggregate being maintained solely by the doubly bridging thiolate and triply bridging chalcogenide ligands. The molecular structure can be described in various ways which emphasize its several geometrical relationships with other structures. Thus **3M**(**4M**) is (a) composed of four fused adamantanoid cages, (b) composed of concentric regular and semiregular polyhedra, *octahedro*-M_6-*tetrahedro*-E_4-*truncated tetrahedro*-$(\mu\text{-SR})_{12}$-*tetrahedro*-M_4-*tetrahedro*-$(SR)_4$, (c) a supertetrahedron of 10 vertex-linked coordination tetrahedra, and (d) a symmetrical molecular fragment of the cubic metal chalcogenide lattice.

Although unique, **3M** (**4M**) is structurally comparable with three different aggregates. The cation $[Cd_{10}(SCH_2CH_2OH)_{16}]^{4+}$ [10] has a related molecular structure, with triply bridging thiolate ligands in place of the chalcogenide ions, and with all ligand hydroxyl functions coordinated to eight of the cadmium atoms (one at each of four of the six Cd_{inner} and three at each of the four Cd_{outer}). The compound $Ag_3B_5S_9$ contains supertetrahedral $[B_{10}S_{16}(S_{1/2})_4]^{6-}$ units linked at all four corners.[35,36] Further, the $[Sn_{10}O_4S_{20}]^{8-}$ molecular anion, occurring as hydrated salts with Cs^+ or Na^+, contains the same supertetrahedron $Sn_{10}S_{20}$, but with four additional oxygen atoms arrayed as a tetrahedron and inside each of the four fused adamantane moieties. The oxygen atoms are not centered in the adamantane units, but are bonded only to the inner tin atoms, which thereby acquire SnS_4O_2 coordination.[35,37]

The structural relationship between $[S_4M_{10}(SPh)_{16}]^{4-}$ (**3M**) and $[SM_8(SPh)_{16}]^{2-}$ (**6M**, the hypothetical analogue of **7**), both with idealized symmetry T_d (ignoring substituents), is that both have an outer $(MSR)_4$ tetrahedron connected by four sets of three doubly bridging thiolates to an inner polyhedron of metal atoms. The inner section is either an M_6 octahedron with four faces capped by sulfide (**3M**) or an M_4 tetrahedron centered with a single sulfide (**6M**). As a consequence of these differing inner metal polyhedra, the 12 connecting thiolates constitute either a truncated tetrahedron (**3**) or an icosahedron (**6**).[38] The SM_8S_{16} core of **6M** is not a fragment of a known metal sulfide lattice.

Four equivalent hexagonal faces (**8**) comprise the surface of the supertetrahedral structure **3M** (**4M**), each face being equivalent to three fused M_3S_3 rings in chair conformation. The substituents R at the six peripheral doubly bridging thiolates may be axial or equatorial to the face. However, they are sufficiently separated from each other that contiguous axial pairs of substituents have small (but unambiguous when R = Ph) mutual repulsions. The occurrence in structure A of three axial phenyl substituents adjacent around the periphery of **8**, together with the

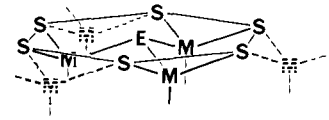

8

occurrence of three axial phenyl groups on one M_3S_3 face of the $[Fe_4(SPh)_{10}]^{2-}$ adamantane structure,[8] confirms that there is limited steric crowding on the face of the supertetrahedron, an observation which has two significant implications. One is that a similar substituent could radiate from the central chalcogenide ion of **3** and **4**, and therefore uncharged molecules $M_{10}(SR)_{20}$ (**9**) or $M_{10}(SeR)_4(SR)_{16}$ (**10**) are feasible. It is known[39] that

(26) Bowmaker, G. A.; Dobson, B. C. *J. Chem. Soc., Dalton Trans.* **1981**, 267.
(27) Band gaps (eV) are ZnS 3.8, ZnSe 2.8, CdS 2.6, CdSe 1.8. Duffy, J. A. *J. Phys. C* **1980**, *13*, 2979.
(28) The full stoichiometries of reactions 5 and 6 have not been reported.
(29) Garner, C. D., private communication.
(30) Shaw, R. A.; Woods, M. *J. Chem. Soc. A* **1971**, 1569. This, the first stage of the "doctor" process, is not surprising because excess thiolate is absent.
(31) Coucouvanis, D.; Swenson, D.; Stremple, P.; Baenziger, N. C. *J. Am. Chem. Soc.* **1979**, *101*, 3392.
(32) A product of the reaction of dibenzyl trisulfide with $[Zn(SPh)_4]^{2-}$ is tentatively identified as $[(PhS)_2ZnS_2Zn(SPh)_2]^{4-}$. Detering, B. A.; Coucouvanis, D.; Patil, P.; Stremple, P.; Dragonjac, M. "Abstracts of Papers", *185th* National Meeting of the American Chemical Society, Seattle, WA, March 1983; American Chemical Society: Washington, DC, 1983; INOR 171.
(33) Coucouvanis, D. *Prog. Inorg. Chem.* **1979**, *26*, 301.
(34) Fitzpatrick, L. J.; Foley, R.; Dance, I. G., unpublished results.
(35) Krebs, B. *Angew. Chem., Int. Ed. Engl.* **1983**, *22*, 113.
(36) Krebs, B.; Diercks, H. *Acta Crystallogr., Sect. A* **1975**, *A31*, S66.
(37) Schiwy, W.; Krebs, H. *Angew Chem., Int. Ed. Engl.* **1975**, *14*, 436.
(38) An S_{12} cuboctahedron also is possible in **6** and **7**. Dance, I. G., to be published.
(39) Schwarzenbach, G.; Gautschi, K.; Peter, J.; Tunaboylu, K. *Trans. R. Inst. Technol. Stockholm* **1972**, *271*, 295.

$[Cd_{10}(SCH_2CH_2OH)_{16}]^{4+}$ in solution reacts with excess thiolate, which could generate $Cd_{10}(SCH_2CH_2OH)_{20}$. The other implication is that there is space for reaction to occur at the face-central chalcogenide ion in **3** and **4**. Face **8** represents the smallest portion of the surface of metal chalcogenide, ME, with one accessible reaction site, and therefore presents a homogeneous model system for surface phenomena on cubic metal chalcogenide.

In this context we point out that the structure we have discovered is but the first and smallest member of an unlimited series of molecular, supertetrahedral fragments of the cubic sphalerite lattice. The thiolate ligands in **3** (**4**) function as termini at the edges and vertices of the supertetrahedron, without disruption of the molecular lattice structure or modification of the metal coordination stereochemistry, and the thiolate ligands do not affect the faces. Therefore larger supertetrahedral fragments of sphalerite can also be terminated in the same fashion to form hypothetical but legitimate macromolecules. The next member

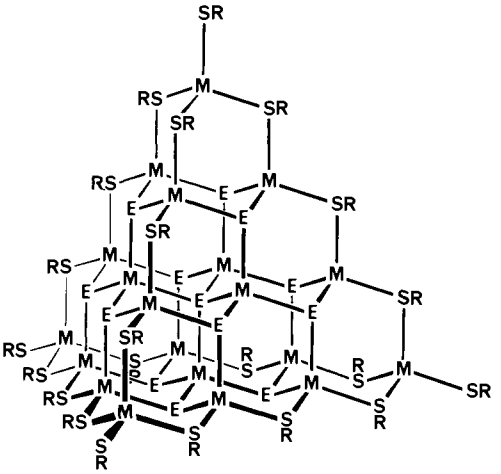

11

of this series of supertetrahedra would be $[E_{13}M_{20}(SR)_{22}]^{8-}$ (**11**), structurally $[(\mu_4\text{-E})(\mu_3\text{-E})_{12}(\mu\text{-SR})_{18}M_{20}(SR)_4]$, in which there is only one structural element not present in **3** (**4**), namely the tetrahedrally coordinated central chalcogenide ion, which is the predominant component of bulk metal chalcogenide. In considering the possibility of the existence and isolation of **11**, it should be noted that its charge density would be 0.24 e^- per surface E or S atom, which is greater than the corresponding value (0.20 e^- per E, S) in **3** (**4**). This should stabilize **11** with respect to degradation to metal chalcogenide, and in view of the stability of **3** in this regard, augurs well for the preparation of macromolecules of type **11**.

Analogous fragments of the hexagonal (wurtzite) metal chalcogenide structure, terminated with thiolate ligands, are not as readily conceivable. The difficulty arises at the M_3S_3 cycles in boat conformation and requires introduction of $(\mu_3\text{-SR})_2M(SR)_2$ building units, for which there is no precedent in polymetallic thiolate cages.

The structure of **3M** (**4M**) is fundamentally different from the structures of the iron and cobalt species $[S_wM_x(SR)_y]^{z-}$ and from the structures of sulfido–metal–phosphine clusters such as $[E_2Ni_3(PEt_3)_6]^{2+}$,[40,41] $[S_9Ni_9(PEt_3)_6]^{2+}$,[42] $[S_6Fe_8(PEt_3)_8]^{2+}$,[43] $[S_8Co_6(PEt_3)_6]^{+,2+}$,[44,45] all of which have the M_2S_2 rhombus as the fundamental structural unit. Structure **3M** is instead derived from M_3S_3 cycles in chair conformation. This differentiation is not simply a function of the metal and its contribution to the electron population or the possibility of direct bonding between metal atoms, because M_3S_3 cycles occur also in the adamantane structure **2M** with Mn,[28] Fe, Co, Zn, and Cd. Structure **7M** is composed of larger M_4S_4 cyclic units.

Finally we reiterate the theme of the structural congruence of *molecular* chalcogenide–metal–thiolates and *nonmolecular* metal chalcogenides, which underlies much of the above discussion and provides direction and incentive for further research. In broad terms, this view of corresponding structures is comparable with that[46] of large metal cluster molecules as fragments of bulk metal, terminated by carbon monoxide or other ligands,[47,48] and with that of metal alkoxides as models for metal oxides.[49,50]

Acknowledgment. This research is supported by The Australian Research Grants Scheme. We thank D. C. Craig for diffractometry and A. D. Rae for contributions to the isomer analysis.

Registry No. 2Cd, 91670-05-2; **2Zn**, 76915-21-4; **3Cd**, 84493-86-7; **3Zn**, 84507-22-2; **4Cd**, 91686-32-7; **4Zn**, 91670-07-4; $(Me_4N)_2[Zn(SPh)_4]$, 76915-22-5; $(Me_4N)_2[Cd(SPh)_4]$, 82677-50-7; benzenethiol, 108-98-5.

Supplementary Material Available: Listings of d-spacings and relative intensities for lines in polycrystalline diffraction patterns of **2Zn**, **2Cd**, **3Cd** (crystal structure A), and **3Zn** (crystal structure B/C); atomic, positional, and thermal parameters for crystal structures A, B, and C; listings of $10|F_o|$ and $10|F_c|$ for crystal structures A, B, and C (30 pages). Ordering information is given on any current masthead page.

(40) Ghilardi, C. A.; Midollini, S.; Sacconi, L. *Inorg. Chim. Acta* **1978**, *31*, L431.
(41) Cecconi, F.; Ghilardi, C. A.; Midollini, S. *Cryst. Struct. Commun.* **1982**, *11*, 25.
(42) Ghilardi, C. A.; Midollini, S.; Sacconi, A. *J. Chem. Soc., Chem. Commun.* **1981**, 47.
(43) Cecconi, F.; Ghilardi, C. A.; Midollini, S. *J. Chem. Soc., Chem. Commun.* **1981**, 640.
(44) Cecconi, F.; Ghilardi, C. A.; Midollini, S. *Inorg. Chim. Acta* **1982**, *64*, L47.
(45) Cecconi, F.; Ghilardi, C. A.; Midollini, S.; Orlandini, A. *Inorg. Chim. Acta* **1983**, *76*, L183.
(46) Chini, P. *J. Organomet. Chem.* **1980**, *200*, 37.
(47) "Transition Metal Clusters"; Johnson, B. F. G., Ed.; Wiley: New York, 1980.
(48) Johnson, B. F. G.; Lewis, J. *Adv. Inorg. Chem. Radiochem.* **1981**, *24*, 225.
(49) Chisholm, M. H.; Huffman, J. C.; Kirkpatrick, C. C.; Leonelli, J.; Folting, K. *J. Am. Chem. Soc.* **1981**, *103*, 6093.
(50) Chisholm, M. H.; Folting, K.; Huffman, J. C.; Rothwell, I. P. *J. Am. Chem. Soc.* **1982**, *104*, 4389.